

Nitrous oxide emissions from aerobic granular sludge

Lydia Jahn, Karl Svardal  and Jörg Krampe 

ABSTRACT

The emissions of climate-relevant nitrous oxides from wastewater treatment with aerobic granular sludge (AGS) are of special interest due to considerable structural as well as microbiological differences compared with flocculent sludge. Due to the compact and large structures, AGS is characterised by the formation of zones with different dissolved oxygen (DO) and substrate gradients, which allows simultaneous nitrification and denitrification (SND). N₂O emissions from AGS were investigated using laboratory-scale SBR fed with municipal wastewater. Special attention was paid to the effects of different organic loading rates (OLR) and aeration strategies. Emission factors (EF) were in a range of 0.54% to 4.8% (gN₂O/gNH₄-N_{ox}) under constant aerobic conditions during the aerated phase and different OLR. Higher OLR and SND were found to increase the N₂O emissions. A comparative measurement of two similarly operated SBR with AGS showed that the reactor operated under constant aerobic conditions (DO of 2 mg L⁻¹) emitted more N₂O than the SBR with an alternating aeration strategy. Total nitrogen (TN) removal was significantly higher with the alternating aeration since non-aerated periods lead to increased anoxic zones inside the granules. The constant aerobic operation was found to promote the accumulation of NO₂-N, which could explain the differences in the N₂O levels.

Key words | aerobic granular sludge, N₂O emission, nitrogen removal, SBR

Lydia Jahn (corresponding author)
Karl Svardal 
Jörg Krampe 
Institute for Water Quality and Resource
Management,
TU Wien,
Karlsplatz 13/226-1, 1040 Vienna,
Austria
E-mail: ljahn@iwag.tuwien.ac.at

INTRODUCTION

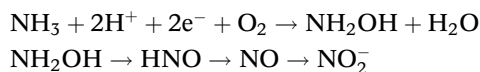
Today's focus in wastewater treatment plant (WWTP) operation moves towards sustainable treatment and low greenhouse gas emissions. In this regard, special attention is paid to N₂O formation during biological wastewater treatment. Relevant pathways for N₂O formation in wastewater treatment are described by Wunderlin *et al.* (2012) as well as by Kampschreur *et al.* (2009). The most relevant mechanism for N₂O production was reported with the autotrophic nitrification pathway. During nitrification, ammonium is oxidised to hydroxylamine and in a further step to nitrite. Hereby it is assumed that incomplete hydroxylamine oxidation is responsible for the N₂O release. The rate of the incomplete hydroxylamine oxidase reaction increases when both NH₄-N and NO₂-N concentrations

are elevated. Another pathway for the formation of N₂O is the so-called nitrifier denitrification. In the absence of oxygen, ammonium-oxidising bacteria (AOB) can no longer transfer part of the electrons from nitrite to the oxygen and therefore not only produce NO₂⁻ as an end product, but also N₂O, NO and N₂. Furthermore, N₂O is a by-product of the denitrification process and produced during the conversion of nitrate to nitrogen. High N/COD ratios (COD: chemical oxygen demand) can promote N₂O formation due to incomplete denitrification. Moreover, since the N₂O reductase is sensitive to oxygen, micro-aerobic conditions (low dissolved oxygen (DO)) during denitrification can promote N₂O formation too. The following equations describe the formation pathways through nitrification, nitrifier denitrification and heterotrophic denitrification. Further less relevant formation pathways for N₂O are found in the literature as chemo-denitrification and dissimilatory nitrate-ammonification (Chalk & Smith 1983; Tallec *et al.* 2008; Hu *et al.* 2011).

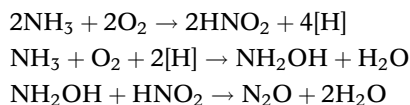
This is an Open Access article distributed under the terms of the Creative Commons Attribution Licence (CC BY-NC-ND 4.0), which permits copying and redistribution for non-commercial purposes with no derivatives, provided the original work is properly cited (<http://creativecommons.org/licenses/by-nc-nd/4.0/>)

doi: 10.2166/wst.2019.378

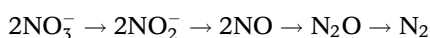
Nitrification:



Nitrifier denitrification:



Heterotrophic denitrification:



Although a high number of publications focus on the emissions of climate-relevant N_2O from conventional activated sludge systems, only a few studies relate to the emissions from aerobic granular sludge (AGS). [Table 1](#) summarises N_2O emission factors (EF) of different AGS studies as well as measurements from conventional full-scale WWTP with suspended activated sludge. The EF of these studies appear in a broad range, which is probably attributed to the different operational strategies. [Quan *et al.* \(2012\)](#) found increased EF under lower aeration rates and limited carbon availability. The authors claimed that elevated N_2O emissions might be due to structural reasons and an increased SND for aerobic granules with larger diameter. [Lochmatter *et al.* \(2013\)](#) investigated the nitrogen removal and N_2O emissions of AGS under different aeration strategies and COD loads (constant nitrogen load). The highest EF of 9.0% was measured under the lowest COD load and under alternating high/low DO. Lower N_2O emissions of 2.1% and 1.0% occurred at higher COD loads (C/N ratios). [Van den Akker \(2015\)](#) determined

N_2O emissions of an AGS system operated with high saline municipal wastewater in a range of 2.3% to 6.8%. The lowest N_2O emissions were measured when nitrite and ammonium were consumed and the DO in the bulk liquid was above 1.0 mg L^{-1} ([van den Akker *et al.* 2015](#)). Similar findings were made by [Peng *et al.* \(2018\)](#), whereby decreased DO levels promoted SND and subsequently increased N_2O emissions. However, low DO levels are required to achieve maximum SND, indicating that there has to be a compromise between nitrogen removal and N_2O emissions.

[Parravicini *et al.* \(2015\)](#) as well as [Foley *et al.* \(2010\)](#) investigated the N_2O emissions of full-scale conventional WWTP and found EF up to approximately 1.5%. [Table 1](#) demonstrates that the EF of AGS systems are overall higher compared with full-scale measurements on conventional WWTP. It can be supposed that results from laboratory-scale cannot be directly compared with full-scale measurements, which is probably due to different reactor geometry and aeration rates. Since AGS is dominated by larger sizes ($>200 \mu\text{m}$), the compact structure promotes the formation of zones with different DO and substrate levels. In contrast to suspended activated sludge, where the bulk liquid concentrations of the substrate and DO are similar in all zones, AGS is characterised by gradients, which lead to the formation of intermediates in different layers.

In regard to the structural differences of AGS compared with conventional sludge flocs and the formation of zones with different DO, several N_2O formation pathways can coexist within the biomass ([Lochmatter *et al.* 2013](#)) and illustrate that the emissions of climate-relevant N_2O out of AGS deserve further research. The complexity of the different formation pathways for N_2O during biological wastewater treatment indicates the difficulty of quantifying the impact of operational settings, especially the aeration strategy. Further research is needed in order to understand the different

Table 1 | Literature review on N_2O emissions of AGS and conventional WWTP with suspended activated sludge

Reference	EF [%]	Referring to	Scale
Aerobic granular sludge			
Lochmatter <i>et al.</i> (2013)	1.0–9.0	TN_{IN}	Laboratory-scale
van den Akker <i>et al.</i> (2015)	2.3–6.8	TN_{IN}	Pilot-scale
Quan <i>et al.</i> (2012)	2.2–8.2	TN_{IN}	Laboratory-scale
Gao <i>et al.</i> (2016)	2.72 ± 0.52	$\text{NH}_4\text{-N}_{\text{ox}}$	Laboratory-scale
Zhang <i>et al.</i> (2015)	7.0–21.9	TN_{rem}	Laboratory-scale
Suspended activated sludge			
Parravicini <i>et al.</i> (2015)	0.002–1.52	TN_{IN}	Full-scale
Foley <i>et al.</i> (2010)	0.006–0.253	TN_{rem}	Full-scale

triggers for N₂O formation, which allows setting arrangements for declining emissions from biological wastewater treatment. This study focused on N₂O emissions in correlation with different aeration strategies and organic loading rates (OLR) of AGS operated with municipal wastewater.

METHODS

SBR setup

AGS was cultivated in two laboratory-scale SBR with a volume of 6 to 8 L. After 261 days (data points 1 to 6), the reactors were restarted and operated again for 240 days (data points 7 and 8). The first experimental phase includes measurements under different OLR, while during the second period different aeration strategies were investigated. The operation comprised an anaerobic plug-flow feed of 60 to 90 min. Cycles lasted 4 to 6 h with settling times between 1 and 10 min. The exchange ratios were 30% to 40%. Temperatures and pH values were monitored daily as well as sludge volume measurements. SBR were fed with sewage from a municipal WWTP. Table 2 shows the relevant concentrations of the wastewater during the measurements. COD was mostly between 230 and 530 mg L⁻¹ with total nitrogen (TN) concentration between 28 and 50 mg L⁻¹. N/COD ratios were in a range of 0.08 to 0.18. The samples for the sequencing were collected on day 501 (second period).

The different settling properties were attributed to a slightly diverse reactor operation. The applied settling

times affected the minimum settling velocities ($v_{s,min}$), which were in a range of 0.7 to 3.2 m h⁻¹. The minimum settling velocity is described as the quotient of the drawn water level and the settling time and determines the slow settleable substances that are discharged with the effluent. Samples 4 and 5 had a high SV₁₀/SV₃₀ ratio compared with the other measurements, which were attributed to a low $v_{s,min}$ of approximately 0.7 m h⁻¹ and a reduced washout of flocculent sludge. Although the biomass was occasionally dominated by flocculent structures, there were large granules with sizes above 200 µm present in the SBR during all measurements.

During the off-gas sampling, bulk liquid samples were taken in regular intervals for analysing NH₄-N, NO₂-N, and NO₃-N according to DIN 38406. The formation of anoxic zones within the biomass depends on the granule sizes and the DO level in the bulk liquid. Smaller sizes limit the formation of anoxic zones and thus the ability for SND. COD and mixed liquor suspended solids were measured according to DIN 38409. Based on the distribution of the nitrogen fractions, simultaneous nitrogen removal was calculated according to the following equation (Zhang et al. 2015):

$$\text{SND} = \frac{\text{NH}_4^+ \text{ oxidised} - \text{NO}_x^- \text{ accumulated}}{\text{NH}_4^+ \text{ oxidised}} \times 100 \%$$

The microbial community was investigated by Illumina MiSeq sequencing Nextera XT library, 341F – 802R primers. It should be noted that *Nitrobacter* may well be present, however *Nitrospira* is not always detected by Illumina MiSeq sequencing.

Table 2 | Wastewater composition, cycle operation and settling properties during different measurements

	1	2	3	4	5	6	7	8
SBR	2	2	2	1	1	1	1	2
Day	80	101	110	198	205	260	501	501
Wastewater composition								
COD [mg L ⁻¹]	448	283	309	244	470	530	228	228
TN [mg L ⁻¹]	45.6	50.2	39.3	28.0	48.0	42.8	34.7	34.7
TP [mg L ⁻¹]	9.2	10.6	11.4	15.3	17.7	11.2	5.8	5.8
Cycle time [min]	240	240	240	240	240	240	360	360
Anaerobic [min]	60	60	60	90	90	90	90	90
Settling [min]	2	3	3	10	10	2	10	10
Decant [min]	5	5	5	5	5	5	5	5
SVI [ml g ⁻¹]	69.2	78.1	89.6	64.3	75.9	64.1	47.8	70.3
SV ₁₀ /SV ₃₀ [-]	1.10	1.07	1.26	1.35	1.84	1.66	1.17	1.17
$v_{s,min}$ [m h ⁻¹]	3.21	2.89	2.28	0.69	0.77	2.82	0.84	0.84

Gas probes

The SBR were completely covered during the aerated phase, while sampling the exhaust air. Gas chromatography–mass spectrometry (GC-MS) was used for the N₂O analysis of the gas samples. Exhaust air samples from the SBR were injected into 20 ml sealed and evacuated headspace gas bottles by means of a gas-tight glass syringe. The sample amount was 10 ml. For the GC-MS, a Porapak column (ID 0.32 mm and length about 30 m) was used. The headspace gas cylinders filled with the exhaust air samples were analysed immediately or stored in a thermostat at 20 °C until analysis to avoid temperature fluctuations. Gas samples with N₂O contents between 0.5 and 40 ppmv were used for the validation of the GC-MS measurement for N₂O according to DIN 32645. Moreover, the validation parameters including detection and determination limit as well as the standard deviation were determined. N₂O samples were analysed to check the zero point. According to DIN 32645, a detection limit (DL₁) of 0.5 ppmv, a determination limit (DL₂) of 1.0 ppmv and the standard deviation of 0.56 ppmv were calculated. These values are even lower (DL₁ = 0.25 ppmv, DL₂ = 0.50 ppmv) when the usual ‘signal to noise’ ratio (S/N) in chromatography is considered (Kromidas 2011).

For the evaluations, the measured ppmv in the exhaust air was converted to the concentration of N₂O as gram per litre air. To compare the results, the gas volume was adjusted to standard temperature. During the sampling, the aeration intervals were recorded to calculate the N₂O load emitted from the reactor per cycle. For this calculation, the required aeration rate was checked in preparation for the measurements. EF were related to the oxidised NH₄-N according to the following equation:

$$EF = \frac{\sum (Q_{\text{air}} \cdot C_{\text{N}_2\text{O,air}})}{Q_{\text{Feed}} \cdot \text{NH}_4^+ \text{ oxidised} \left[\frac{\text{gN}_2\text{O}}{\text{gNH}_4\text{-N}} \right]}$$

Respiration tests

Oxygen utilisation rates for carbon and nitrogen (OUC, OUN) were determined by respiration tests. OUC was determined without the use of ATU (allylthiourea, nitrifier inhibitor) since the sludge was afterwards returned to the reactor. OUC was measured at the end of the cycle to guarantee that the nitrogen respiration was zero. In contrast, the highest oxygen utilisation rate was measured at the beginning of the aerated phase, when

nitrogen was in a range of 5 to 10 mg L⁻¹. OUN was calculated with the following equations considering the measured temperatures. Oxygen utilisation rates were needed to create COD and nitrogen mass balances.

$$\text{OUC}_{t20} = \text{OUC}_t \cdot 1.072^{(20-t)}$$

$$\text{OU}_{t20,\text{max}} = \text{OU}_t \cdot 1.103^{(20-t)}$$

$$\text{OUN}_{t20} = \text{OU}_{t20,\text{max}} - \text{OUC}_{t20}$$

RESULTS AND DISCUSSION

Upstart and operation

The reactors were inoculated with a mixture of AGS from an earlier phase and suspended activated sludge from a municipal WWTP. Minimum settling velocity was 6 m h⁻¹ during the first 50 days. The sludge volume index (SVI) of both SBR was 94 ml g⁻¹ in the beginning of the tests. SVI of SBR 1 decreased to 67 ml g⁻¹ within 23 days and fluctuated between 60 to 80 ml g⁻¹ until day 64. Due to a technical failure, a great amount of sludge of SBR 1 was lost at day 74, thus, the results of the following 5 weeks were excluded from the evaluation. Until the end of the first phase (day 261), the SVI of SBR 1 ranged again between 61 and 79 ml g⁻¹. Similar results during the startup were observed for SBR 2. SVI declined to 60 ml g⁻¹ within 18 days. The average sludge loading during the first phase was 0.34 gCOD gTSS⁻¹ d⁻¹. Both SBR were aerated to a DO in the range of 1.8 to 2.2 mg L⁻¹ without anoxic conditions in the bulk liquid. The operation of SBR 2 included a stirrer during non-aerated phases, which probably caused increased shear stress and SVI in a range of 64 to 97 ml g⁻¹. From day 119 on, the SVI of SBR 2 climbed up to 300 ml g⁻¹, which was attributed to the growth of filaments. SBR 2 was no longer sampled for N₂O under these unstable conditions.

During the second startup with activated sludge from a municipal WWTP, $v_{s,\text{min}}$ of both reactors was increased to approximately 4 m h⁻¹ by reducing the settling time from 6 to 3 min. Stirrers were not used during these experiments. SVI declined to 42 (SBR 1) and 48 ml g⁻¹ (SBR 2) within 35 days. For both reactors, SVI was between 40 and 60 ml g⁻¹ until day 91. Since a high amount of suspended solids was present in the effluent, the settling time was enlarged and $v_{s,\text{min}}$ decreased to approximately 1.4 m h⁻¹. Between the tests, there were elevated NO_x-N concentrations measured in both reactors and mean-time high SVI up to 100 ml g⁻¹. However, compact granules with sizes above 200 μm were

observed by regular microscopy. A recirculation of purified water through the settled sludge bed was applied to improve TN removal. With this strategy, it was possible to reduce the $\text{NO}_x\text{-N}$ concentration to approximately 5 to 10 mg L^{-1} , which ensured again anoxic-anaerobic feeding conditions and declining SVI. N_2O sampling was performed at the end of the phase (day 501), when SVI and $\text{NO}_x\text{-N}$ concentration were in a representative range. The average OLR during the second phase was $0.25 \text{ gCOD gTSS}^{-1} \text{ d}^{-1}$.

Mass balance

Figure 1 shows the calculated COD and nitrogen mass balances exemplary for data point 1. The calculations consider the input and output loads to the SBR during the measured cycle as well as the carbon and nitrogen respiration rates. The balances were calculated for the cycles with N_2O sampling according to the following equations.

COD balance:

$$\text{OUC} = \text{COD}_{\text{IN}} + \text{COD}_{\text{XA}} - \text{COD}_{\text{OUT}} - \Delta\text{COD}_{\text{SP}} [\text{mg}]$$

$$\text{OUC} = \text{COD}_{\text{IN}} + 0.3(\text{N}_{\text{TN,IN}} - \text{N}_{\text{NH}_4\text{-N,OUT}}) - \text{COD}_{\text{OUT}} - Y_{\text{BM}} \cdot (\text{COD}_{\text{IN}} - \text{COD}_{\text{OUT}}) [\text{mg}]$$

Nitrogen balance:

$$\text{N}_D = \text{N}_{\text{TN,IN}} + \text{N}_{\text{NO}_x\text{-N,IN}} - \text{N}_{\text{NH}_4\text{-N,OUT}} - \text{N}_{\text{NO}_x\text{-N,OUT}} - \Delta\text{N}_{\text{NO}_x\text{-N}} - \text{N}_{\text{N}_2\text{O}} [\text{mg}]$$

The sludge production was determined with a biomass yield (Y_{BM}) of $0.25 \text{ gTSS gCOD}^{-1}$ ($0.3 \text{ gCOD gCOD}^{-1}$). Since there was no sludge removed during the cycle, the biomass growth is presented as $\Delta\text{COD}_{\text{SP}}$. COD_{XA} is the COD

load produced through the autotrophic growth of the nitrifiers due to biomass cell synthesis of CO_2 and assumed as 30% of the oxidised nitrogen load. Oxygen utilisation for carbon removal (OUC) was calculated with the measured carbon respiration (OUC_{CO_2}) as well as with the oxygen gained through denitrification. The oxygen utilisation (OUC_{O_2}) was related to the entire aerobic phase and the reactor volume. The deviation was referred to the input COD and amounted to 6.3%. Other data were checked according to the procedure and deviations were found up to 12%.

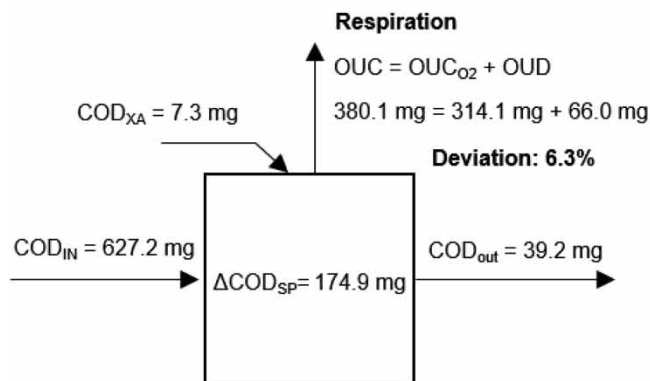
The nitrogen mass balances were calculated with the in- and output nitrogen loads and the $\text{NO}_x\text{-N}$ left over from the previous cycles. The oxygen utilisation rate for nitrogen (OUN) during the aerated cycle was measured as 29.3 mgO_2 , which is close to the theoretical OUN calculated based on the oxidised ammonium loads. The difference in the OUN was found to be 1.8% and up to 10% for all measurements.

Effect of organic loading rate

Since SND is a promising ability of aerobic granules, the first tests focused on the operation under fully aerobic conditions during the aerated phase without anoxic periods in the bulk liquid. DO was throughout adjusted to 2 mg L^{-1} with aeration rates of 2 L min^{-1} . Under these conditions, the effect of different OLR on the N_2O emissions from AGS was investigated including seven measurements (data points 1 to 7). OLR ranged between 0.13 and $0.42 \text{ gCOD gTSS}^{-1} \text{ d}^{-1}$. Temperatures were in a range between 21.2 and 24.0°C . $\text{NH}_4\text{-N}$ removal reached 66.0% and 99.4%, while TN removal was calculated as 41.6% to 78.5%.

Figure 2 shows the nutrients and N_2O levels for data points 3 and 5 during the aerated phase. Generally, it was

COD balance



N balance

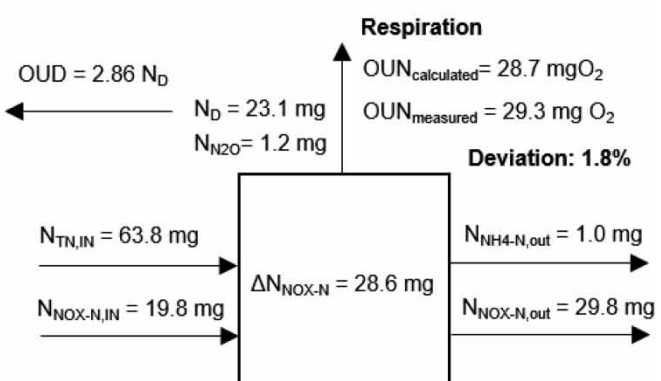


Figure 1 | COD (left) and nitrogen mass balance (right) for data point 1.

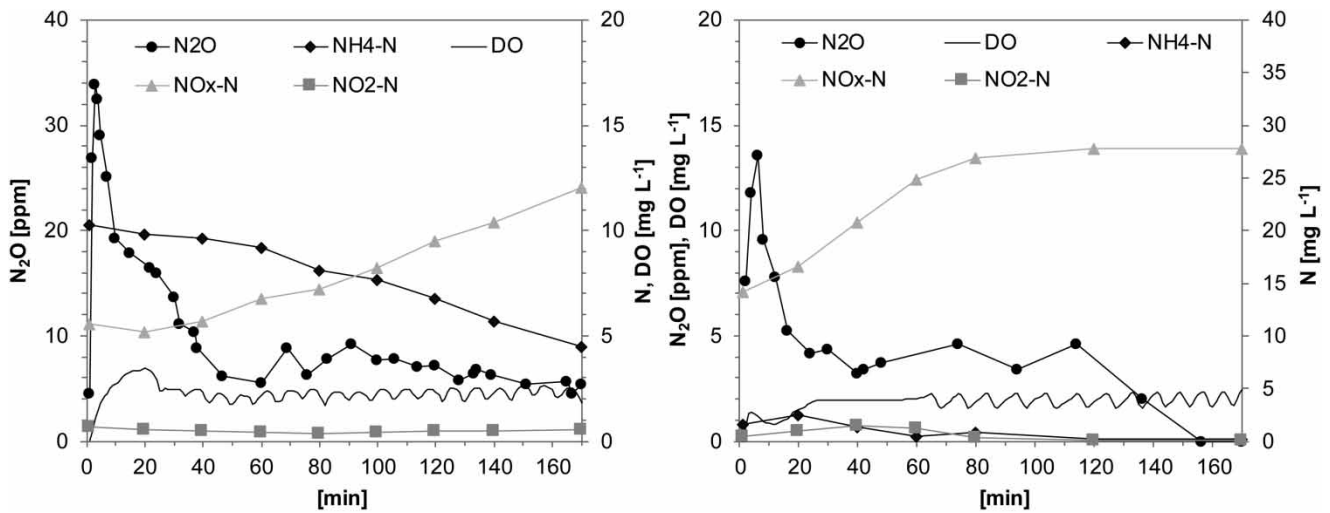


Figure 2 | N_2O , $\text{NH}_4\text{-N}$, $\text{NO}_2\text{-N}$, $\text{NO}_x\text{-N}$ and DO during the aerated cycle for data points 3 (left) and 5 (right).

found, that the measured $\text{NH}_4\text{-N}$ concentrations were approximately 25% lower than the theoretical $\text{NH}_4\text{-N}$ concentration that should be measured after feeding. We assume that this fact was due to $\text{NH}_4\text{-N}$ adsorption on the granules as it was reported by Bassin et al. (2011). The authors observed an increased adsorption capacity of AGS compared with activated sludge, with an $\text{NH}_4\text{-N}$ adsorption in a range of 23% to 36% at 20 °C. During all measurements, the highest N_2O levels in the off-gas were measured at the beginning of the aerated phase with the highest substrate availability. The N_2O peaks appeared within the first 5 min with N_2O levels mostly between 10 and 35 ppm. This is in line with findings from van den Akker et al. (2015), who observed N_2O peaks in the exhaust air during the changeover from the anaerobic feed to the aerated phase, which was probably

associated with an increased oxygen uptake and lower DO levels during the first few minutes of aeration. N_2O emissions steadily decreased afterwards, whereby the emissions were almost zero after all $\text{NH}_4\text{-N}$ was oxidised (Figure 2, right). Since there was no full $\text{NH}_4\text{-N}$ removal achieved during run 5, N_2O was also present at the end of the aeration with off-gas concentrations of approximately 5 ppm (Figure 2, left).

Figure 3 (left) shows the EF under different OLR, which were calculated in a range of 0.54% to 4.8% ($\text{N}_2\text{O}/\text{NH}_4\text{-N}_{\text{ox}}$). During the tests, nitrite was identified as a relevant trigger for increased N_2O emissions and an indicator for elevated AOB activity. Clearly increased N_2O emissions appeared for data points 6 and 7 (triangle), whereby enhanced nitrite levels of 3.3 and 4.8 mg L^{-1} were detected within the aerated phase. During runs 1 to 5 (dots), the nitrite

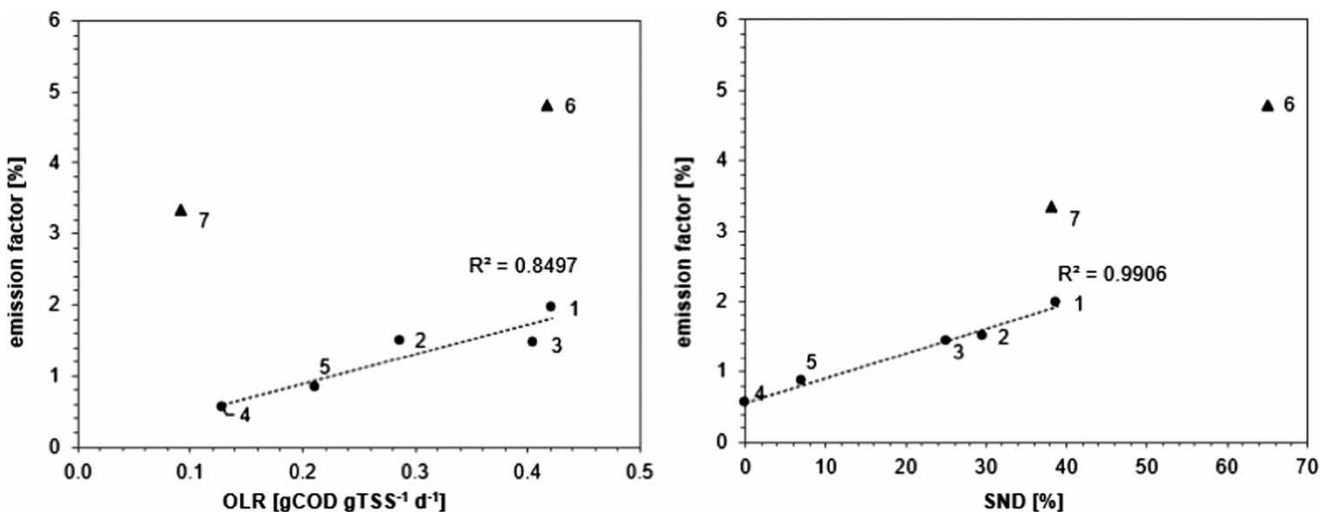


Figure 3 | OLR to EF (left) and SND to EF (right) for the tests with fully aerobic conditions during aeration [dots: $\text{NO}_2\text{-N} < 1.8 \text{ mg L}^{-1}$, triangle: $\text{NO}_2\text{-N} > 3.0 \text{ mg L}^{-1}$].

concentrations were much lower at 0.7 and 1.8 mg L⁻¹. Overall, the results indicate that higher OLR lead to increased EF, which is in line with an earlier study from Guo *et al.* (2017). The authors investigated the N₂O emissions from an SBR operated with AGS under different food/microorganism (F/M) ratios and found EF between 2.77% and 3.79%. In the study of Guo *et al.* (2017), the increased F/M ratios led to decreased DO levels (approximately 1 mg L⁻¹). In this case, the OLR was increased and the DO decreased, which promotes N₂O formation from autotrophic nitrification and nitrifier denitrification. Especially during the beginning of the aeration, when the oxygen uptake is the highest, the nitrifier denitrification pathway could contribute to increased N₂O emissions. It has to be mentioned that municipal WWTP are normally operated with OLR between 0.05 and 0.15 gCOD gTSS⁻¹ d⁻¹. In this loading range, the N₂O emissions of our presented data are below 1%, which fits to EF measured at full-scale municipal WWTP (Parravicini *et al.* 2015).

A further correlation of the present study was found between the EF and the amount of SND (Figure 3, right). SND was detected especially in the beginning of the aeration (within the first 20 min) and was probably linked to a high oxygen uptake and increased anoxic zones inside the granules. SND decreased afterwards, since oxygen penetrated into deeper zones. In that case, the granule size plays a key role in the formation of anoxic zones. Furthermore, the DO and substrate diffusion into the granules are limited by larger diameter. The measurements were performed over a period of a half year, during which differences in the granulation grade probably affected the SND capacity. Low emissions were found for data points 4 and 5, where the low SND capacity was attributed to an increased flocculent proportion. Gao *et al.* (2016) found increased EF from AGS operated under SND and claimed that the AOB and heterotrophic denitrifiers are responsible for the N₂O emissions. The authors suggested that when the external COD is depleted, the internally stored substrate is used as electron donor for incomplete denitrification, which leads to an increased N₂O formation due to heterotrophic denitrification. Moreover, a large granule size and a subsequently limited COD diffusion into the granules can be further reasons for elevated N₂O emissions. Stewart (2003) summarised different diffusion coefficients for various substrates. Hereby, the nitrogen and oxygen diffusion coefficients for temperatures of 25 °C were reported in a similar range with 18.8·10⁻⁶ and 20·10⁻⁶ cm² s⁻¹. Lower diffusion coefficients were reported for carbon sources like glucose and acetic acids within a range of 6.7·10⁻⁶ cm² s⁻¹

to 12.1·10⁻⁶ cm² s⁻¹. A limited carbon diffusion into the granules could promote N₂O formation via heterotrophic denitrification in combination with SND. Findings from Lochmatter *et al.* (2013) verify our assumption of limited carbon availability, since the authors found lower N₂O emissions with higher COD loads under constant NH₄-N inflow concentrations. A further trigger for N₂O formation over heterotrophic denitrification is the presence of oxygen during denitrification. Since SND relates to oxygen gradients in the biomass, micro-aerobic conditions can affect the N₂O reductase and therefore increase N₂O emissions (Lemaire *et al.* 2006).

In summary, we suggest that the OLR affects N₂O formation in different ways. Firstly, increased loads lead to enhanced AOB activity and N₂O formation from autotrophic nitrification especially at the beginning of the aeration. SBR operation includes a period feed, thus, high NH₄-N levels appear in the beginning of the aeration and decline afterwards by nitrification. Moreover, the higher OLR probably leads to an increased oxygen uptake through the outer zones, which causes enlarged anoxic zones inside the granules. This would explain the increased SND activity and N₂O formation from heterotrophic denitrification.

Moreover, AGS systems are operated with an anaerobic feeding strategy to enrich substrate-storing organisms, that take up most of the incoming COD during the feed. Denitrifying phosphate and glycogen accumulating organisms (PAO and GAO) play an important role in partial denitrification. Earlier studies state that denitrification by GAO and PAO can cause increased N₂O emission (Zeng *et al.* 2003a, 2003b; Lemaire *et al.* 2006; Kampschreur *et al.* 2009). The metabolism of these organisms is associated with growth on storage compounds, in which PHB consumption is the rate-limiting step. Schalk-Otte *et al.* (2000) observed elevated N₂O emissions when PHB was the substrate to grow during COD limitation. Phosphate uptake in the presented study ranged from 0 to 0.96 gP gTSS⁻¹, which indicates that PAO activity was different during the measurements. However, it was found that higher EF appeared when the phosphate uptake was increased. The impact of enhanced biological phosphate removal of AGS on N₂O emissions should be addressed in further research.

Effect of aeration strategy

Over a period of 240 days after the restart, the two SBR were operated in parallel to investigate the effect of different aeration strategies on nitrogen removal. The simultaneous sampling for both SBR was conducted to identify which

aeration strategy is more decisive for N_2O formation. The aeration control setting for SBR 1 ensured continuous aerobic conditions during the aerated phase with DO levels between 1.8 and 2.2 mg L^{-1} . For SBR 2, an alternating aeration was applied with a 5 min aeration interval to a DO level of 2 mg L^{-1} that was followed by a 5 min aeration pause. N_2O emissions of the two SBR were measured under similar operating conditions. Both SBR were fed with the same municipal wastewater and an OLR of 0.1 $\text{gCOD gTSS}^{-1} \text{d}^{-1}$. The N/COD ratio was 0.15 and thus in an optimal range. N/COD ratios above 0.15 indicate COD limitations. The aeration rates were set to 2 L min^{-1} for both reactors. TSS in the SBR were similar at 3.0 and 3.3 g L^{-1} respectively.

Figure 4 shows the $\text{NH}_4\text{-N}$ and TN removal of both SBR over the second experimental phase. At some points, there was no full $\text{NH}_4\text{-N}$ removal achieved for SBR 1. This was mainly due to increased loading rates and a meantime growth of *Arcella* (days 385 to 430), which was observed by regular microscopy. Unfortunately, it was not possible to identify the reasons for the development of *Arcella* in SBR 1. Increased OLR of 0.6 $\text{gCOD gTSS}^{-1} \text{d}^{-1}$ appeared for SBR 1 during days 311 and 318 and caused a decline in $\text{NH}_4\text{-N}$ removal. TN removal for SBR 1 was mostly between 50% and 60%. With the applied aeration strategy for SBR 2, complete $\text{NH}_4\text{-N}$ removal was recorded over the entire period. TN removal increased until day 501 to approximately 90%, which can be attributed to larger granule sizes growing with time and enlarged anoxic zones for denitrification.

Figure 5 shows the course of N_2O emissions in the exhaust air and the nutrients over the aerated cycle. N_2O sampling occurred on day 501 simultaneously for both

reactors. $\text{NH}_4\text{-N}$ concentrations were similar during the start of the aeration at 7.5 mg L^{-1} (SBR 1) and 7.9 mg L^{-1} (SBR 2). The highest emissions were measured at the beginning of the sampling. With the onset of aeration, the off-gas concentrations increased to 55 ppm N_2O (SBR 1) and 70 ppm N_2O (SBR 2). Up to this time, the $\text{NH}_4\text{-N}$ uptake rate of SBR 1 was almost twice that of SBR 2. Within the first 20 min, the $\text{NH}_4\text{-N}$ concentrations were reduced to 2.5 and 5.4 mg L^{-1} resulting in ammonia-oxidising rates of 5.1 (SBR 1) and 2.8 $\text{mg NH}_4\text{-N gTSS}^{-1} \text{h}^{-1}$ (SBR 2). N_2O levels decreased with declining $\text{NH}_4\text{-N}$ concentrations. However, for SBR 1 the N_2O emissions increased again after approximately 20 min of aeration, which was probably linked to a rising $\text{NO}_2\text{-N}$ level (3.88 mg L^{-1}). In contrast, $\text{NO}_2\text{-N}$ was nearly stable for SBR 2 at 1.2 to 1.8 mg L^{-1} . EF for SBR 1 and SBR 2 were calculated at 3.32% and 1.62% ($\text{N}_2\text{O}/\text{NH}_4\text{-N}_{\text{ox}}$). Besides increased AOB activity, the different EF can be attributed to the different $\text{NO}_2\text{-N}$ concentrations within the aerated phase. Zeng *et al.* (2003a) assumed that nitrous oxide reductase is inhibited by nitrite concentrations above 1 mg L^{-1} . This reported $\text{NO}_2\text{-N}$ level was clearly exceeded in both reactors. However, the periods without aeration (SBR 2) probably allowed denitrification of $\text{NO}_2\text{-N}$ and subsequently lower N_2O emissions compared with SBR 1.

The results illustrate that the main source of N_2O was related to autotrophic nitrification since the emissions clearly correlated to the ammonium oxidation. N_2O was no longer detectable when ammonium was depleted. Total $\text{NH}_4\text{-N}$ removal was found for SBR 1 and 2 to be 99.0% and 99.6%. TN removal reached 69.2% for SBR 1 with constant aerobic aeration, while SBR 2 achieved a TN removal

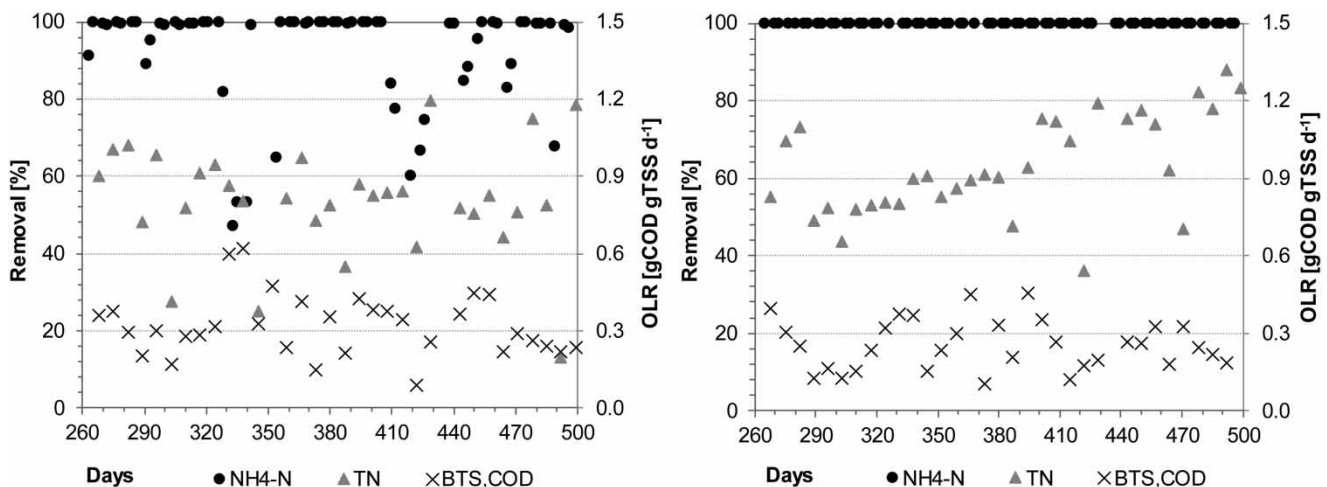


Figure 4 | OLR, $\text{NH}_4\text{-N}$ and TN removal for SBR 1 (left) and SBR 2 (right).

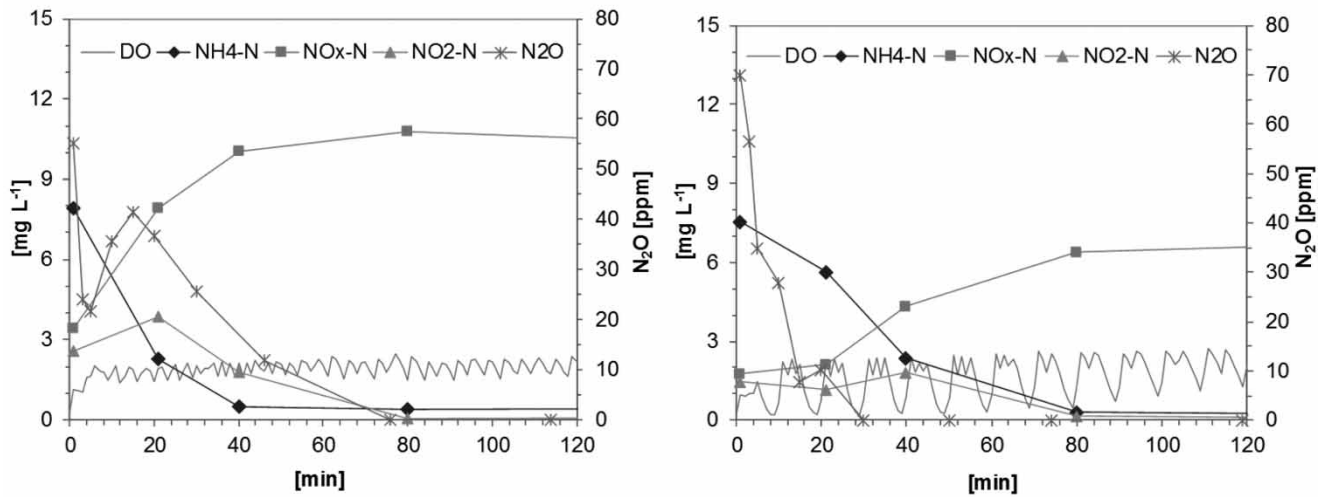


Figure 5 | $\text{NH}_4\text{-N}$, $\text{NO}_x\text{-N}$, $\text{NO}_2\text{-N}$ and DO in the liquid phase and N_2O in the exhaust air of SBR 1 and 2.

of 77.30% with an alternating aeration mode. The results are in line with Lochmatter *et al.* (2013), where higher TN removal was found with an alternating aeration mode. In this study, the constant DO also amounted to higher $\text{NO}_2\text{-N}$ emissions compared with the alternating aeration strategy. Zhang *et al.* (2015) observed higher N_2O emissions in a fully aerobic SND compared with the aerobic-anoxic SND by inhibition tests and reported an increased nitrifier denitrification as the main source for N_2O . However, with our applied method we cannot prove the presence of nitrifier denitrification, even though it has been mentioned as a relevant N_2O formation pathway in biofilms (Schreiber *et al.* 2009). Since it is known that nitrifier denitrification is mainly related to oxygen-limited conditions, we assume that N_2O formation from nitrifier denitrification could appear temporarily within the beginning of the aeration due to an increased oxygen uptake in the outer zone of the granules.

Figure 6 shows the microbial community of the investigated AGS (taxonomy, phylum, class) of the two SBR. The taxonomic distributions of the communities were quite similar. An increased abundance of the phylum *Parcubacteria* was found for SBR 2. Since these bacteria were mostly observed under anoxic conditions (Castelle *et al.* 2017), we assume that the increased proportion of *Parcubacteria* in SBR 2 was related to increased anoxic conditions due to non-aerated periods. Since N_2O is an intermediate of the metabolism of the involved nitrifying and denitrifying bacteria, the microbial composition of AOB and NOB effects the N_2O formation mainly. Winkler *et al.* (2015) investigated the correlation between the involved microorganisms and the nitrite accumulation by

modeling and experimental tests and revealed that *Nitrobacter* was the dominant NOB in aerobic granules and not *Nitrospira*. The authors claimed that in AGS systems NOB grow uncoupled from AOB, which can lead to additional nitrite formation due to partial denitrification by *Nitrobacter*. Although the microbial community of the present study was also characterised by an elevated NOB/AOB ratio, *Nitrobacter* was not detectable; instead *Nitrospira* was found to be the dominant NOB in both SBR, which is also in line with findings from earlier AGS studies (Thwaites *et al.* 2017). NOB/AOB ratios determined by gene sequencing were 1.2 (SBR 1) and 1.7 (SBR 2), respectively, and thus increased compared with a reported NOB/AOB ratio of approximately 0.2 (± 0.1) for a conventional treatment plant (Winkler *et al.* 2012). Although an increased growth of NOB is coupled to the accumulation of nitrite, elevated NOB/AOB ratios were also found in correlation with increased temperatures and decreasing DO, which illustrates that further parameters affect the presence of nitrifying and denitrifying bacteria.

CONCLUSION

Due to the structural properties of AGS, the bacterial community and the arrangement of individual microorganisms are quite different compared with conventional activated sludge. Several triggers for N_2O formation in AGS systems were identified in the framework of this study. The evaluated data reveal a correlation between the OLR and the SND in the N_2O emissions and were identified as relevant triggers for N_2O formation.

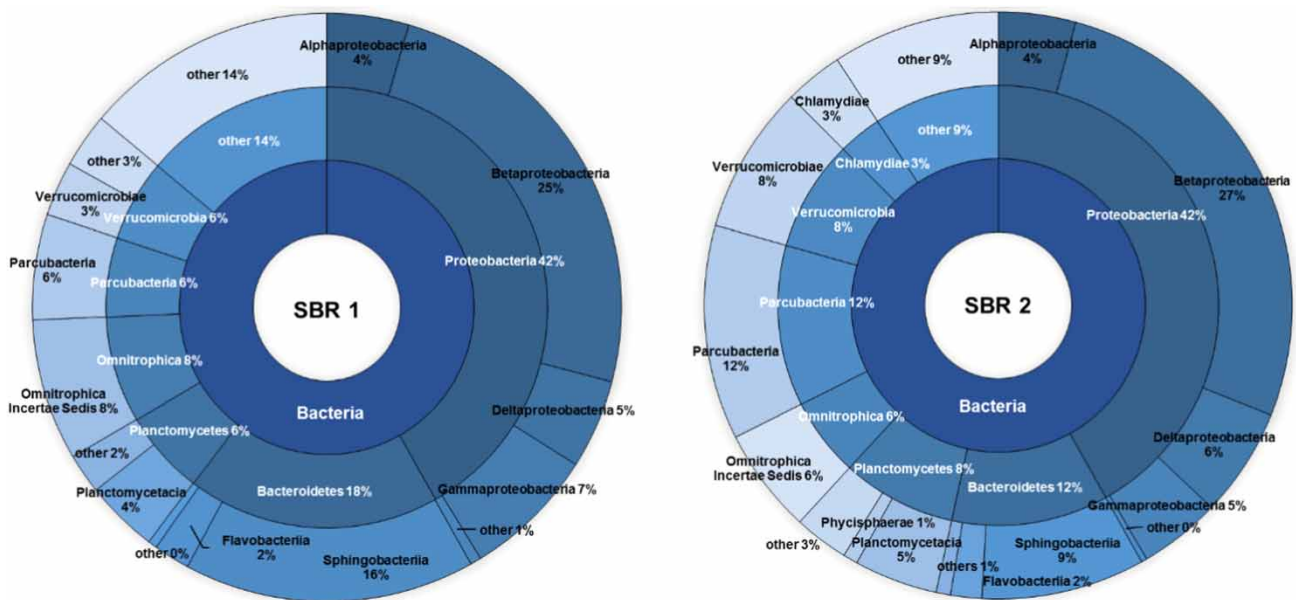


Figure 6 | Microbial community of the AGS (taxonomy, phylum, class) by Illumina MiSeq sequencing.

Increased loads promote N_2O formation via autotrophic nitrification and probably due to nitrifier denitrification since, at the beginning of the aerated phase, higher loads lead to higher DO uptake through the outer layers. Furthermore, the increased OLR promote SND and N_2O formation via heterotrophic denitrification, which is probably a reason for endogenous denitrification and COD limitation. EF under fully aerobic conditions during the aerated phase were calculated in a range of 0.54% to 4.8% at OLR between 0.13 and $0.42 \text{ gCOD gTSS}^{-1} \text{ d}^{-1}$. This aeration strategy was found to promote nitrite accumulation and increased N_2O emissions. It has to be taken into account that nitrite is a sign of high AOB activity and can have a direct impact on N_2O formation. The alternating aeration strategy was found to be more efficient for TN removal and lower N_2O emissions. Against the background of desired low N_2O emissions, the alternating aeration strategy with anoxic-aerobic conditions should be favored for the operation of AGS systems.

ACKNOWLEDGEMENTS

This work was carried out as part of the research project 'KontiGran', which was supported by the Austrian Federal Ministry of Sustainability and Tourism.

REFERENCES

- Bassin, J. P., Pronk, M., Kraan, R., Kleerebezem, R. & van Loosdrecht, M. C. M. 2011 Ammonium adsorption in aerobic granular sludge, activated sludge and anammox granules. *Water Res.* **45** (16), 5257–5265.
- Castelle, C. J., Brown, C. T., Thomas, B. C., Williams, K. H. & Banfield, J. F. 2017 Unusual respiratory capacity and nitrogen metabolism in a Parcubacterium (OD1) of the Candidate Phyla Radiation. *Sci. Rep.* **7**, 40101.
- Chalk, P. M. & Smith, C. J. 1983 Chemodenitrification. In: *Gaseous Loss of Nitrogen from Plant–Soil Systems* (J. R. Freney & J. R. Simpson, eds), Springer, Dordrecht, The Netherlands, pp. 65–89.
- Foley, J., de Haas, D., Yuan, Z. & Lant, P. 2010 Nitrous oxide generation in full-scale biological nutrient removal wastewater treatment plants. *Water Res.* **44** (3), 831–844.
- Gao, M., Yang, S., Wang, M. & Wang, X. H. 2016 Nitrous oxide emissions from an aerobic granular sludge system treating low-strength ammonium wastewater. *J. Biosci. Bioeng.* **122** (5), 601–605.
- Guo, N., Zhang, J., Xie, H.-J., Tan, L.-R., Luo, J.-N., Tao, Z.-Y. & Wang, S.-G. 2017 Effects of the food-to-microorganism (F/M) ratio on N_2O emissions in aerobic granular sludge sequencing batch airlift reactors. *Water* **9** (7), 477.
- Hu, Z., Zhang, J., Xie, H., Li, S., Zhang, T. & Wang, J. 2011 Identifying sources of nitrous oxide emission in anoxic/aerobic sequencing batch reactors (A/O SBRs) acclimated in different aeration rates. *Enzyme Microb. Technol.* **49** (2), 237–245.
- Kampschreur, M. J., Temmink, H., Kleerebezem, R., Jetten, M. S. M. & van Loosdrecht, M. C. M. 2009 Nitrous oxide emission during wastewater treatment. *Water Res.* **43** (17), 4093–4103.

- Kromidas, S. 2011 *Validierung in der Analytik (Validation in Analytics)*. Wiley-VCH, Weinheim, Germany.
- Lemaire, R., Meyer, R., Taske, A., Crocetti, G. R., Keller, J. & Yuan, Z. 2006 Identifying causes for N₂O accumulation in a lab-scale sequencing batch reactor performing simultaneous nitrification, denitrification and phosphorus removal. *J. Biotechnol.* **122** (1), 62–72.
- Lochmatter, S., Gonzalez-Gil, G. & Holliger, C. 2013 Optimized aeration strategies for nitrogen and phosphorus removal with aerobic granular sludge. *Water Res.* **47** (16), 6187–6197.
- Parravicini, V., Valkova, T., Haslinger, J., Saracevic, E., Winkelbauer, A., Tauber, J., Svardal, K., Hohenblum, P., Clara, M., Windhofer, G., Pazdernik, K. & Lampert, C. 2015 *ReLaKO-Reduktionspotential bei den Lachgas-Emissionen aus Kläranlagen durch Optimierung des Betriebes*. Bundesministerium für Land- und Forstwirtschaft, Umwelt und Wasserwirtschaft, Vienna, Austria.
- Peng, B., Liang, H., Wang, S. & Gao, D. 2018 Effects of DO on N₂O emission during biological nitrogen removal using aerobic granular sludge via shortcut simultaneous nitrification and denitrification. *Environ. Technol.*, doi: 10.1080/09593330.2018.1494757.
- Quan, X., Zhang, M., Lawlor, P. G., Yang, Z. & Zhan, X. 2012 Nitrous oxide emission and nutrient removal in aerobic granular sludge sequencing batch reactors. *Water Res.* **46** (16), 4981–4990.
- Schalk-Otte, S., Seviour, R. J., Kuenen, J. G. & Jetten, M. S. M. 2000 Nitrous oxide (N₂O) production by *Alcaligenes faecalis* during feast and famine regimes. *Wat. Res.* **34** (7), 2080–2088.
- Schreiber, F., Loeffler, B., Polerecky, L., Kuypers, M. M. M. & de Beer, D. 2009 Mechanisms of transient nitric oxide and nitrous oxide production in a complex biofilm. *ISME J.* **3** (11), 1301–1313.
- Stewart, P. S. 2003 Diffusion in biofilms. *J. Bacteriol.* **185** (5), 1485–1491.
- Tallec, G., Garnier, J., Billen, G. & Gossiaux, M. 2008 Nitrous oxide emissions from denitrifying activated sludge of urban wastewater treatment plants, under anoxia and low oxygenation. *Bioresour. Technol.* **99** (7), 2200–2209.
- Thwaites, B. J., Reeve, P., Dinesh, N., Short, M. D. & van den Akker, B. 2017 Comparison of an anaerobic feed and split anaerobic–aerobic feed on granular sludge development, performance and ecology. *Chemosphere* **172**, 408–417.
- van den Akker, B., Reid, K., Middlemiss, K. & Krampe, J. 2015 Evaluation of granular sludge for secondary treatment of saline municipal sewage. *J. Environ. Manage.* **157**, 139–145.
- Winkler, M. K. H., Bassin, J. P., Kleerebezem, R., Sorokin, D. Y. & van Loosdrecht, M. C. M. 2012 Unravelling the reasons for disproportion in the ratio of AOB and NOB in aerobic granular sludge. *Appl. Microbiol. Biotechnol.* **94** (6), 1657–1666.
- Winkler, M. K. H., Le, Q. H. & Volcke, E. I. P. 2015 Influence of partial denitrification and mixotrophic growth of NOB on microbial distribution in aerobic granular sludge. *Environ. Sci. Technol.* **49** (18), 11003–11010.
- Wunderlin, P., Mohn, J., Joss, A., Emmenegger, L. & Siegrist, H. 2012 Mechanisms of N₂O production in biological wastewater treatment under nitrifying and denitrifying conditions. *Water Res.* **46** (4), 1027–1037.
- Zeng, R. J., Lemaire, R., Yuan, Z. & Keller, J. 2003a Simultaneous nitrification, denitrification, and phosphorus removal in a lab-scale sequencing batch reactor. *Biotechnol. Bioeng.* **84** (2), 170–178.
- Zeng, R. J., Yuan, Z. & Keller, J. 2003b Enrichment of denitrifying glycogen-accumulating organisms in anaerobic/anoxic activated sludge system. *Biotechnol. Bioeng.* **81** (4), 397–404.
- Zhang, F., Li, P., Chen, M., Wu, J., Zhu, N., Wu, P., Chiang, P. & Hu, Z. 2015 Effect of operational modes on nitrogen removal and nitrous oxide emission in the process of simultaneous nitrification and denitrification. *Chem. Eng. J.* **280**, 549–557.

First received 6 May 2019; accepted in revised form 1 November 2019. Available online 11 November 2019